J. exp. Biol. 156, 187–205 (1991)
Printed in Great Britain © The Company of Biologists Limited 1991

THE KINEMATICS AND PERFORMANCE OF THE ESCAPE RESPONSE IN THE ANGELFISH (*PTEROPHYLLUM EIMEKEI*)

BY PAOLO DOMENICI AND ROBERT W. BLAKE

Department of Zoology, University of British Columbia, Vancouver, BC, Canada V6T 2A9

Accepted 13 November 1990

Summary

The kinematics of turning manoeuvres and the distance–time performance in escape responses of startled angelfish (*Pterophyllum eimekei*) are investigated employing high-speed cinematography (400 Hz). All escape responses observed are C-type fast-starts, in which the fish assumes a C shape at the end of the initial body contraction (stage 1). Kinematic analysis of the subsequent stage (stage 2) allows the response to be classified into two types: single bend (SB), in which the tail does not recoil completely after the formation of the C, and double bend (DB), in which it does.

The two types of response have different total escape angles (measured from the subsequent positions of the centre of mass, SB 120.0°; DB 73.3°, $P<0.005$), different stage 2 turning angles (in the same direction as stage 1 for SB, 11.0°; in the direction opposite to stage 1 for DB, −21.9°: $P<0.0005$) and different maximum angular velocities in the direction opposite to the initial one (SB $-8.08\,rad\,s^{-1}$; DB $-56.62\,rad\,s^{-1}$: $P<0.001$). There are no significant differences in stage 1 kinematics for the two types of escape. Stage 1 turning angle is linearly correlated to stage 2 turning angle for DB only ($P<0.01$; $r^2=0.60$) and to total escape angle for both types of response ($P<0.0001$; $r^2=0.80$). Stage 1 duration is linearly correlated to stage 1 turning angle ($P<0.0001$; $r^2=0.83$) and to total escape angle ($P<0.0001$; $r^2=0.72$) for both types of escape.

Distance–time performance is also different in the two response types, mainly because of differences in stage 2 (maximum velocity for SB $0.99\,m\,s^{-1}$; maximum velocity for DB $1.53\,m\,s^{-1}$: maximum acceleration for SB $34.1\,m\,s^{-2}$; maximum acceleration for DB $74.7\,m\,s^{-2}$: $P<0.0001$ in both cases). As a result, there are significant differences in the performance throughout the whole response (maximum velocity $1.02\,m\,s^{-1}$ and $1.53\,m\,s^{-1}$ for SB and DB fast-starts, respectively; maximum acceleration $63.2\,m\,s^{-2}$ and $91.9\,m\,s^{-2}$ for SB and DB fast-starts, respectively) as well as within a fixed time (0.03 s). Overall, higher distance–time performances associated with smaller angles of turn are found in DB than in SB responses.

Key words: angelfish, C-start, kinematics, manoeuvrability, performance, *Pterophyllum eimekei*.

Comparison with previous studies reveals that angelfish have a good fast-start performance despite specializations for low-speed swimming. In addition, the angelfish turning radius ($0.065\pm0.0063L$, where L is body length; mean$\pm$2 S.E.) is lower than that previously reported for any fish.

Introduction

Escape reactions involving fast-start responses allow fish to avoid sudden actual or potential danger in their environment. Fish lacking a fast-start response possess other structural or behavioural antipredator adaptations (e.g. toxins, spines, burrowing habits; Eaton *et al.* 1977; Webb, 1978*a*). The kinematics of the escape response has been shown to be similar for different species of fish (Eaton *et al.* 1977; Webb, 1978*a*). It has been described as a fixed action pattern consisting of a strong unilateral contraction of the body musculature which bends the fish in a C shape (stage 1), followed by a strong propulsive stroke of the tail in the direction opposite to that of the initial contraction (stage 2) (Gillette, 1987). The result is an extremely rapid acceleration of the animal. A third kinematic stage can be present, in which the fish continues to swim or coasts (Weihs, 1973; Webb and Blake, 1985). Previous studies have focused on the first two kinematic stages (see Webb, 1976, 1978*a*; Eaton and Hackett, 1984, for reviews).

The mechanisms mediating stage 1 are relatively well understood (DiDomenico *et al.* 1988; Nissanov and Eaton, 1989). The initial contraction during stage 1 of a C-type fast-start is usually initiated by a single pair of prominent neurones (Mauthner cells), although alternative circuits may exist (Eaton *et al.* 1984; DiDomenico *et al.* 1988). A parallel network of neurones interacting with the Mauthner cells controls the extent of stage 1 contraction (DiDomenico *et al.* 1988). Nothing is known about the mechanisms triggering stage 2.

Adaptations for good fast-start performance are thought to include a large proportion of white muscle (fast-starts are fuelled anaerobically) relative to red, large caudal fin and body depth for producing thrust, and high body flexibility (Weihs, 1973; Blake, 1983; Webb, 1984). The prey's success in escaping predators depends upon its performance (velocity, acceleration) and accurate timing of the reaction (Eaton and Hackett, 1984; Webb, 1976, 1986*b*). In previous studies, much attention has been focused on acceleration performance (Webb, 1976, 1978*a*,*b*; Dubois *et al.* 1976; Harper and Blake, 1990). Manoeuvrability (turning radius, turning angle) has also been suggested to play an important role in predator avoidance (Howland, 1974; Webb, 1976, 1982; Nissanov and Eaton, 1989).

Weihs (1973) hypothesized that body morphology would be a key determinant of maximum acceleration in fish. Previous studies have focused on fusiform fish (Dubois *et al.* 1976; Webb, 1976, 1978*a*, 1986*a*; Eaton *et al.* 1977; Harper and Blake, 1990). The present study investigates how a disc-shaped fish specialized for paired-fin swimming at low speed (Blake, 1979) performs in fast-starts.

Materials and methods

Fish

Angelfish (*Pterophyllum eimekei*, synonymous with *P. scalare*; Schultz, 1967) were obtained from a local (Vancouver, BC) dealer and held in a glass tank (75 cm×40 cm×30 cm) supplied with aerated, dechlorinated water and equipped with a recirculating filter. The water temperature was maintained between 24 and 26°C. The fish were fed pelleted food. Five fish (total length, L=7.26±0.4 cm; mean±2 S.E.) were used in the experiment. Morphological variables are listed in Table 1. The position of the centre of mass (CM) was determined by hanging the killed fish from one point along its body profile. The procedure was repeated for two different points; the crossing point of the two straight lines descending from the hanging points indicated CM. Total wetted surface area (body and median fins) was determined by overlapping a piece of plastic sheet on both sides of the fish and comparing its mass to that of a standard of known area. The percentage of muscle mass was determined by dissection of freshly killed fish (Scale Mettler model PK 300).

Filming procedure

Single fish were transferred to a glass tank (60 cm×32 cm×30 cm) placed in the middle of a larger Plexiglas tank (240 cm×120 cm×45 cm), surrounded by a black plastic screen. The fish could see neither the approaching stimulus nor the investigator. A 2.5 cm grid was placed on the bottom of the tank. Fish were left in the experimental tank for at least 30 min prior to filming.

A plastic container filled with water and suspended adjacent to the arena was thrown against the side of the external tank to elicit the escape responses. A mirror angled at 45° over the tank allowed the top view of the fish to be filmed. The experimental tank was illuminated by two 650 W photographic lights and escaping fish were filmed with a high-speed ciné camera (Locam model 51-0002) on Kodak 7277 4X 400 ASA ciné film at 400 Hz.

Analysis

Twenty sequences were analysed. Processed films were projected on a white panel (55 cm×80 cm), allowing the image to be magnified five times, to minimize measurement error (Harper and Blake, 1989). The position of the 'stretched

Table 1. *Mean morphometric characteristics*

Total length (L) (cm)	Mass (M) (g)	Muscle mass (M_m) (g)	Distance from centre of mass to nose (CM) (cm)	Wetted surface area (S_w) (cm^2)	N
7.26±0.4	8.55±0.86	3.33±0.45	2.69±0.2	53.78±4.9	5
	$0.0223L^3$	$0.389M$	$0.37L$	$1.02L^2$	

Values are mean±2 S.E.

straight' fish centre of mass for the film analysis was determined by aligning a wire, marked at CM, along the midline of the image of the fish. The centre of mass and the tips of the head and tail were recorded frame by frame. These points were later digitized on a digitizing pad (GTCO type, 0.61 m×0.91 m) connected to a computer (80286 AT-compatible). Data were then transferred to an Olivetti M24 PC for further analysis.

The velocity and acceleration data were derived from the raw distance–time data by using a five-point smoothing regression (Lanczos, 1956). Stage 1 (s1) and stage 2 (s2) durations were determined from the change in the direction of displacement of the head. Two types of response were observed: single bend (SB), in which the body did not completely straighten after the initial C bend, and double bend (DB), in which a full return flip of the tail was observed after the initial contraction. The end of stage 2 was not observable for SB responses; in this case, s2 variables were calculated up to eight frames after the end of s1.

Stage 1 turning angle for the anterior part of the body was determined by measuring the angle between the straight lines passing from the centre of mass to the tip of the head at frame 0 and at the end of stage 1. Stage 2 turning angle was measured in the same way, but using the angle between the end of s1 and the end of s2.

A total escape angle of the CM path was also determined. This angle was measured between the initial orientation of the fish and the regression line considering seven positions of the centre of mass about the end of s2 (s2±3 frames).

The angular velocity of the centre of mass was determined using a five-point smoothing regression (Lanczos, 1956) of the original cumulative angle data. The total turning radius (TR) for each escape was calculated employing the mean instantaneous distance moved (d) and the mean instantaneous angle of turn (γ) of the centre of mass throughout stage 1 (Fig. 1). The turning radius is given by:

$$\mathrm{TR} = d/[2\cos(\pi - \gamma)/2] .$$

Sources of error in maximum acceleration data

Film-derived acceleration data are subject to sampling frequency error (SFE, the error due to over-smoothing at low film speed) and measurement error (ME, the error involved in measuring the distance moved) (Harper and Blake, 1989). Harper and Blake (1989) conclude that subcutaneous microaccelerometry should be used to obtain the most accurate measurement of maximum acceleration. The fish employed in this study were too small (7.26±0.4 cm) to implant microaccelerometers.

In this study, a filming rate of 400 Hz and 5× magnification were employed. According to Harper and Blake (1989), the resulting SFE is about 8%. The highest measurement error is below 8%, estimated for the lowest value of maximum acceleration (s2 SB 10.9 m s^{-2}), and is estimated to be less than 5% for all the other maximum acceleration values recorded.

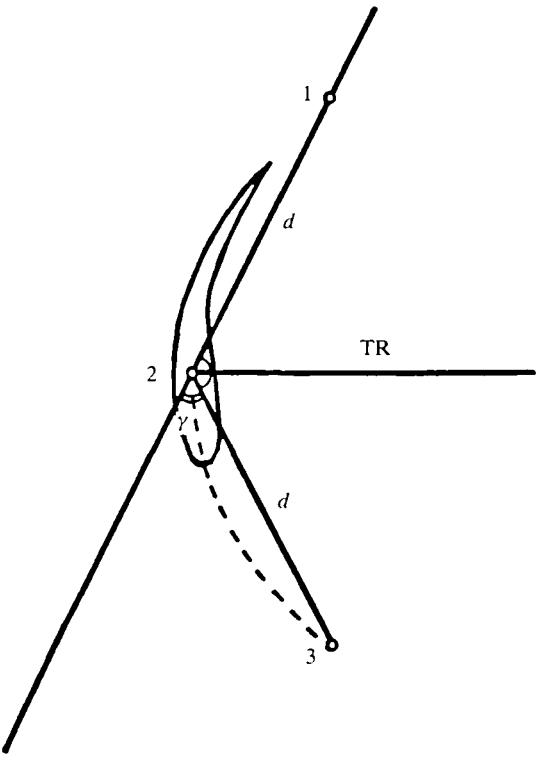

Fig. 1. Turning radius (TR) of an escaping fish. Numbers indicate positions of the centre of mass. Straight lines are drawn from position 1 to position 2 and from position 2 to position 3. The dotted line indicates the path of the centre of mass; d, mean instantaneous distance moved: γ, mean instantaneous angle of turn.

Results

All fast-starts analysed were C-type. Nevertheless, fast-starts can be classified into two main types: single bend (Fig. 2A), in which the tail does not recoil completely after the formation of the C, and double bend (Fig. 2B), showing a clear full return flip during stage 2. The two escape types differ in both turning kinematics and distance–time performance.

Turning kinematics

Turning kinematic parameters are compared for the two types of response in Table 2. There is no significant difference between the s1 turning angles of the two fast-start types. Stage 2 turning angles are statistically different ($P<0.0005$). The mean value of s2 turning angle for SB responses is positive (11.0°), indicating that the turn is continued in the same direction as during s1. However, the mean value of s2 turning angle for DB responses is negative (−21.9°), meaning that the direction of turn is opposite to that in stage 1. This results in the two types showing

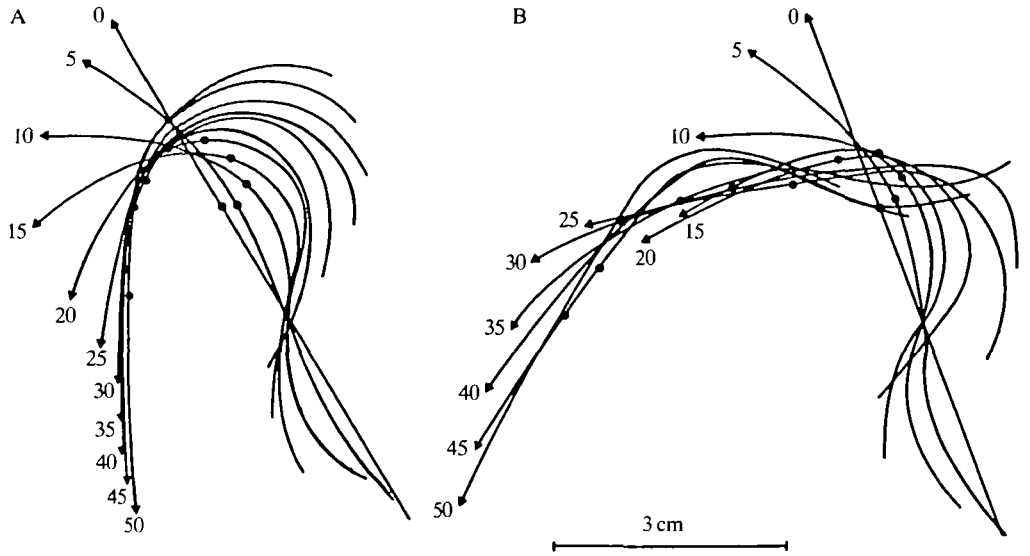

Fig. 2. Tracing of a single bend (A) and a double bend (B) C-start. The midline of the fish and the centre of mass (●) are shown. Numbers indicate time (in ms) and can be matched with Fig. 3A–C.

Table 2. *Turning angles, angular velocity and turning radius for single bend and double bend responses*

	Stage 1 turning angle (degrees)	Stage 2 turning angle (degrees)	Total escape angle (degrees)	Maximum negative angular velocity ($rad\,s^{-1}$)	Turning radius/length	*N*
SB	109.8±16.7	11.0±7.9	120.0±17.5	−8.08±7.75	0.067±0.0075	9
DB	84.6±16.9	−21.9±10.7	73.3±22.1	−56.62±17.98	0.063±0.0098	11
Test	NS	$P<0.0005$	$P<0.005$	$P<0.001$*	NS	
Pooled	95.9±13.0	−7.1±10.1	94.3±17.7	−36.42±15.60	0.065±0.0063	20

t-test is used for all comparisons except those marked with an asterisk (Mann–Whitney).
Values are mean±2 S.E.
NS, not significant; SB, single bend; DB, double bend.

a significantly different total escape angle ($P<0.005$), with a mean value larger than 90° for SB (120°) and smaller for DB (73.3°) responses.

Likewise, the trajectory of the centre of mass changes direction of turn during the DB response. This is reflected in the angular velocity profiles (Fig. 3A). These show a clear change of direction during stage 2 in DB fast-starts, and a gradual decline towards zero in SB fast-starts. The maximum negative angular velocity for

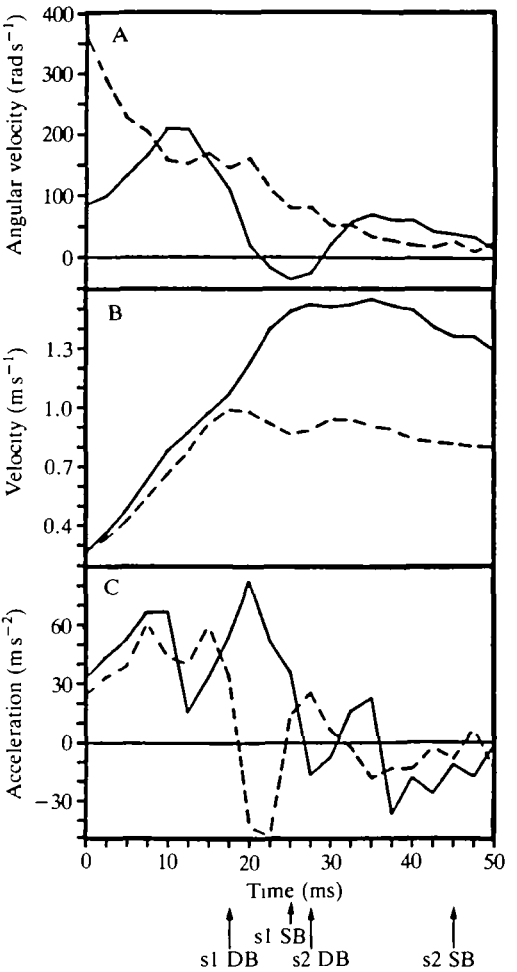

Fig. 3. Angular velocity (A), velocity (B) and acceleration (C) of single bend (SB, dotted line) and double bend (DB, continuous line) C-starts. Times at the completion of stage 1 (s1) and stage 2 (s2) are indicated.

SB responses ($-8.08\,\mathrm{rad\,s^{-1}}$) is statistically different from that for DB responses ($-56.62\,\mathrm{rad\,s^{-1}}$).

The mean value of the turning radius relative to body length is not statistically different between SB ($0.067L$) and DB ($0.063L$) escapes. The pooled mean value is $0.065\pm0.0063L$ (mean±2 S.E.). Stage 1 turning angle is linearly correlated with s2 turning angle only for DB responses ($P<0.01$; Fig. 4A) and s1 turning angles are linearly correlated with the total escape angle for both types. Since the two slopes and elevations are not statistically different, the data have been pooled (Fig. 4B, $P<0.0001$). Stage 1 turning angle and total escape angle are correlated linearly with maximum angular velocity in the direction opposite to the initial one for DB responses only ($P<0.005$ and $P<0.0005$, respectively), whereas the

correlation between s2 turning angle and angular velocity holds for both types, although with different slopes (Fig. 5; SB $P<0.01$; DB $P<0.0001$).

The relative turning radius (TR/L) is not related to any of the performance parameters measured.

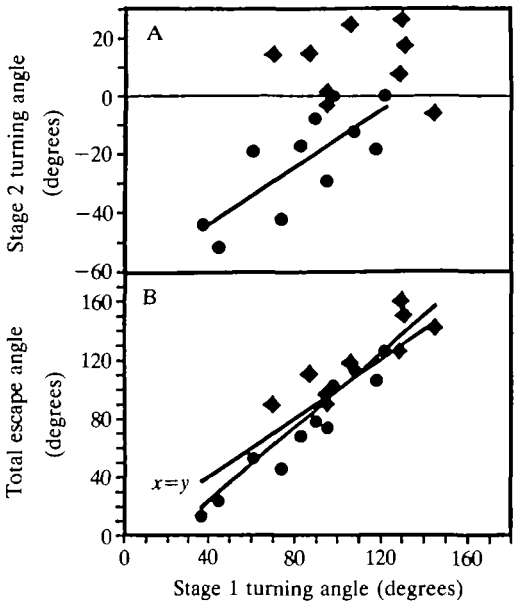

Fig. 4. The relationship of s1 turning angle to s2 turning angle (A) and to total escape angle (B) for single bend (◆) and double bend (●) responses. The linear regression for A ($y=0.49x-63$; $r^2=0.6$; $P<0.01$) is valid for double bend responses only. In B the data are pooled to give the regression line ($y=1.27x-28$; $r^2=0.87$; $P<0.0001$).

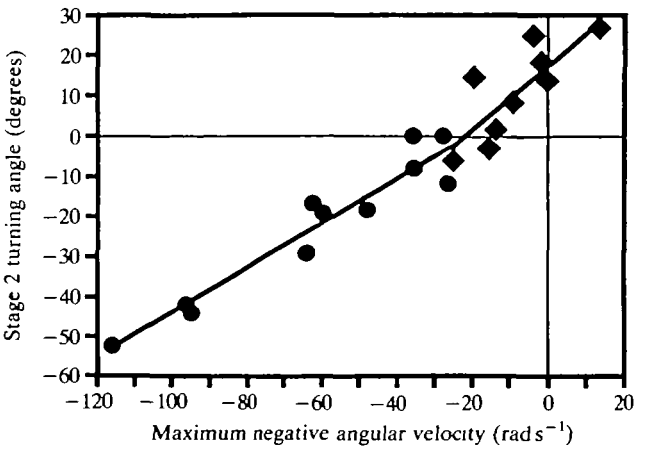

Fig. 5. The relationship between reverse angular velocity and s2 turning angle for single bend (◆) and double bend (●) responses. Linear regressions for single bend ($y=0.80x+18$; $r^2=0.64$; $P<0.01$) and for double bend ($y=0.56x+12$; $r^2=0.92$; $P<0.0001$) responses are shown.

Distance–time performance

Fig. 3B,C shows velocity and acceleration profiles of an SB and a DB escape. The tracings of these two fast-starts are shown in Fig. 2A,B, respectively. The double bend fast-start shows two acceleration peaks of similar magnitude (one in each stage), whereas the single bend fast-start shows high acceleration during s1, followed by lower acceleration during s2 (Fig. 3C). Therefore, after the end of s1, velocity is maintained but not increased in SB responses (Fig. 3B).

The distance–time variables of the two escape types are compared in Table 3, which treats the stages separately. Stage 1 in the two types of response differs significantly in duration (SB 0.023 s; DB 0.017 s; $P<0.005$), distance covered (SB 0.015 m; DB 0.011 m; $P<0.05$), mean acceleration (SB 28.6 m s^{-2}; DB 47.0 m s^{-2}; $P<0.0005$) and maximum acceleration (SB 62.8 m s^{-2}; DB 89.1 m s^{-2}; $P<0.05$). Mean and maximum velocity are not significantly different during s1.

Since no clear end of stage 2 could be established for SB escapes, their s2 duration was considered to be a fixed value (200 ms; eight frames). This is reasonable since, for DB, s2 duration is on average about 80 % that of s1; this corresponds to 7–8 frames for SB. Except for distance covered, all the other distance–time variables are statistically different ($P<0.0001$ in all cases) during s2.

Performance values for s1 and s2 taken together are also summarized in Table 3. Again, except for distance covered, all distance–time variables are statistically different. Overall, the two types of response show a similar performance during stage 1, followed by large differences in stage 2.

In addition, when considering a fixed time interval (30 ms), all the distance–time variables of the two fast-start types are statistically different (Table 3).

Correlations between turning kinematics and performance

Stage 1 turning angle and the total escape angle are linearly correlated with the duration of s1 for both types of response. The data are pooled in Fig. 6A,B, respectively ($P<0.0001$ in both cases), since the slopes and elevations of the regression lines are not statistically different for the two escape types.

No other distance–time variable measured showed any relationship to any of the turning variables within each type of response. However, when turning kinematic data are plotted against distance–time data, the two types of response occupy different regions of the graph. An example is given in Fig. 7, where total maximum velocity is plotted against total escape angle. Single bend and double bend responses occupy the upper left and the lower right parts of the graph, respectively.

Discussion

Turning kinematics

Escape responses in fish are described as consisting of two stages: an initial body bend, in which the fish assumes a C shape, and a subsequent return flip of the tail (Webb, 1976; Eaton and Hackett, 1984). Here, DB responses consist of stages

Table 3. *Results of distance-derived variables during stage 1, stage 2, the total response and the first 0.03 s of the response*

	Duration (s)	Distance (m)	Average velocity ($m s^{-1}$)	Maximum velocity ($m s^{-1}$)	Average acceleration ($m s^{-2}$)	Maximum acceleration ($m s^{-2}$)	*N*
Stage 1							
SB	0.023±0.002	0.015±0.002	0.65±0.05	0.93±0.08	28.6±3.7	62.8±11.1	9
DB	0.017±0.002	0.011±0.002	0.64±0.06	0.98±0.10	47.0±6.3	89.1±13.9	11
t-test	$P<0.005$	$P<0.05$	NS	NS	$P<0.0005$	$P<0.05$	
Pooled	0.020±0.002	0.013±0.002	0.64±0.04	0.96±0.07	38.7±5.6	77.3±10.7	20
Stage 2							
SB	0.020*	0.019±0.002	0.92±0.09	0.99±0.08	−1.8±5.6	34.1±12.7	9
DB	0.014±0.002	0.018±0.002	1.36±0.12	1.53±0.15	37.9±10.0	74.7±7.7	11
t-test		NS	$P<0.0001$	$P<0.0001$	$P<0.0001$	$P<0.0001$	
Pooled	0.017±0.001	0.018±0.001	1.16±0.13	1.29±0.15	20.0±10.8	56.4±11.6	20
Total (s1+s2)							
SB	0.043±0.002*	0.034±0.003	0.77±0.05 (10.8*L*)	1.02±0.09 (14.4*L*)	14.9±3.9	63.2±11.2	9
DB	0.031±0.003	0.029±0.004	0.93±0.05 (12.6*L*)	1.53±0.15 (20.7*L*)	43.2±7.3	91.9±12.8	11
t-test		NS	$P<0.0005$	$P<0.0001$	$P<0.0001$	$P<0.005$	
Pooled	0.036±0.003	0.031±0.003	0.86±0.05 (11.7*L*)	1.30±0.15 (17.8*L*)	30.4±7.8	79.0±10.7	20
Fixed time (0.03 s)							
SB		0.022±0.001	0.71±0.04	1.01±0.08	24.0±5.2	63.0±11.2	9
DB		0.028±0.002	0.92±0.06	1.52±0.15	43.1±6.4	91.9±12.8	11
t-test		$P<0.0001$	$P<0.0001$	$P<0.0001$	$P<0.0005$	$P<0.005$	
Pooled		0.025±0.002	0.83±0.06	1.29±0.14	34.5±6.0	78.9±10.7	20

t-test is used for all comparisons.
* Stage 2 duration is assumed to be 0.02 s for single bend escapes.
Values are mean±2 S.E.
SB, single bend; DB, double bend; NS, not significant; *L*, body length.

described in previous studies (Weihs, 1973; Webb, 1976; Eaton and Hackett, 1984). After the initial turn during s1 (mean angle 84.6°), the head turns in the opposite direction (mean angle −21.9°) as a result of the contralateral body bend. Therefore, the centre of mass undergoes a reversal of its direction of motion (Fig. 3A). The relationship between s2 turning angles and the magnitude of the reversal of angular velocity is shown in Fig. 5.

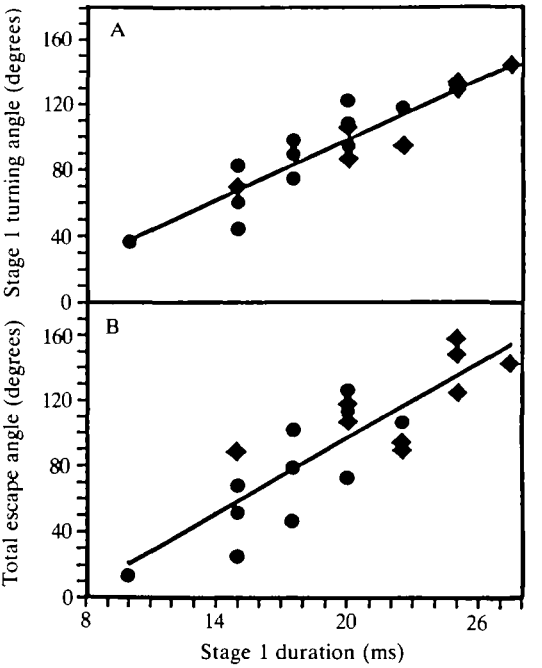

Fig. 6. The relationship between s1 duration and s1 turning angle (A; $y=6.0x-22$; $r^2=0.83$; $P<0.0001$) and total escape angle (B; $y=7.7x-56$; $r^2=0.72$; $P<0.0001$). The regression lines are for single bend (◆) and double bend (●) pooled data.

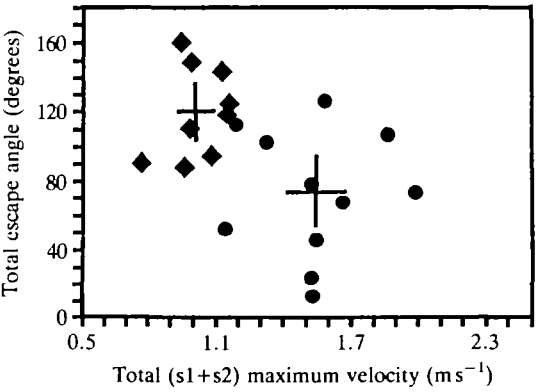

Fig. 7. The relationship between total maximum velocity and total escape angle. Mean ±2 S.E. for single bend (◆) and double bend (●) responses are shown.

In SB escapes the first stage consists of a C bend in which the fish head turns at a mean angle of 109.8°, not statistically different from the angle in a DB escape. Subsequently, the fish straightens, but without bending in the opposite direction. S2 angle is positive on average (+11.0°). As a result, the angular velocity profile of the centre of mass does not show the abrupt decrease typical of DB responses, but slowly decreases towards zero as the centre of mass goes along the tangent of the spiral trajectory (Fig. 3A). The mean total escape angles of the two types of response are different (SB 120.0°; DB 73.3°; $P<0.005$) and they are, respectively, larger and smaller than their corresponding s1 turning angles (SB 109.8°; DB 84.6°). This is because the DB s2 turning angle is in the opposite direction to s1 turning angle, resulting in a more linear trajectory of swimming, whereas the SB s2 turning angle tends to continue the initial turn, producing an overall turning manoeuvre.

Stage 1 angle is related to s2 angle only for DB escapes (Fig. 4A; $P<0.01$; $r^2=0.60$). Eaton *et al.* (1988), in a study on goldfish, found a similar correlation, although their analysis does not discriminate between the two C-start types. This might explain why our slope value (0.49) differs from that of Eaton *et al.* (1988) (1.23), although the *y*-intercepts are similar (−63.3° present study; −59° Eaton *et al.* 1988). Another possibility is that the results of Eaton *et al.* (1988) include both fast-start types. Pooling our data from the two fast-start types, the correlation is still significant ($P<0.01$), although with a lower r^2 value (0.40).

The relationship between s1 and s2 angle is important because it tells us something about how to predict the escape trajectory. Eaton *et al.* (1988) pointed out that because s1 and s2 angles are correlated, the neural commands for the escape trajectory could be organized by the end of stage 1. This relationship does not hold for the current observations on SB responses. However, if the total escape angle is considered, a significant correlation with the s1 turning angle is found for both types. The slopes and elevations of the regressions for the two C-start types are not significantly different, so the data have been pooled to obtain the regression line of Fig. 4B. A line of identity and the regression line cross at 102°. Therefore, below 102°, the total escape angle tends to be smaller than the s1 angle and *vice versa* above 102°. Interestingly, 102° lies between the mean escape angle±2 S.E. for the two types (SB 120°±17.5; DB 73.3°±22.1). Therefore, in SB responses the escape angle increases after stage 1, whereas in DB responses it decreases, resulting in a more linear trajectory of escape. These considerations suggest that s1 turning angle is a better predictor of the actual swimming escape path than it is of s2 turning angle. This is important, because the total escape angle, measured in relation to the swimming path, is probably the most biologically significant angle in terms of predator–prey interactions.

Eaton *et al.* (1988) observed that s1 angles were related to s1 electromyogram (EMG) duration. Our observations, based on film analysis (Fig. 6A), show a similar correlation between s1 angle and s1 duration. Therefore, at least indirectly, s1 duration can predict the total escape angle (Fig. 6B). Since the escape path tends to be away from the stimulus (Blaxter *et al.* 1981; Eaton *et al.* 1981; 80% of

the responses in the present study) and the former is controlled by s1 duration, it might be that some stimulus characteristics (e.g. duration, intensity) influence s1 duration.

It has been suggested that turning radius is a relevant variable in predator–prey interactions (Howland, 1974; Webb, 1976; Weihs and Webb, 1984). Turning radius is thought to be independent of velocity but proportional to length (Howland, 1974). Webb (1976) found this to be the case for trout. Turning radius is independent of velocity for angelfish and is not correlated with any other variable measured. Specific turning radii are $0.067L$ for the SB response and $0.063L$ for the DB response. These values are not statistically different, with an overall mean of $0.065L$, a value significantly lower than those reported in previous studies (Webb, 1976, 1983; Webb and Keyes, 1981). The difference is not surprising because minimum turning radius depends on body flexibility (Aleev, 1969), which, in turn, is a function of the degree of lateral compression. The angelfish is extremely compressed laterally, as can be inferred from the relationship between its total wetted surface area and its length, $S_w=1.02L^2$ ($S_w=0.41L^2$ and $S_w=0.5L^2$ for trout and bass, respectively; Webb, 1983).

Howland (1974) suggests that the relative turning radii of two fish can be predicted if it is assumed that turning moments are generated by lift forces on the body and the caudal fin. Turning radius should then be proportional to the ratio of the mass (M) and the projected lateral area (A_w, sagittal section) and the ratio of the turning radii of two species should be predicted by the ratio of their M/A_w values. For Webb's (1983) trout and bass, we obtain 1.63 for the ratio of the M/A_w values of the two species and 1.77 for the ratio of their turning radii. These values are close, confirming Howland's prediction. However, values of 5.65 for the ratio of the M/A_w values and 9.7 for the ratio of the turning radii are found when comparing the angelfish with trout, and 3.46 and 5.5, respectively, when comparing it with bass. These discrepancies suggest that other force components, especially acceleration reaction (Daniel, 1984) may be more important.

A low value of turning radius can be beneficial in complex environments such as a coral reef or weedy rivers where angelfish live. Although the angelfish keeps its body rigid during routine low-speed locomotion, it is well designed for tight turning manoeuvres during escapes.

Distance-derived performance

The results indicate the presence of two types of C-start associated with different performance levels. Fig. 3C shows that both fast-start types reach high acceleration during s1. Double bend responses show a second peak in acceleration of similar magnitude during s2 and a corresponding increase in velocity (Fig. 3B), whereas for SB responses subsequent acceleration is lower and s1 maximum velocity is barely maintained. As a consequence, although not all distance–time performance values during s1 are significantly different between the two fast-start types, the differences in s2 are such that the overall values of performance throughout the whole response differ significantly (Table 3). In addition, all the

variables measured within a fixed time are significantly larger for DB responses; this includes distance covered, a variable suggested by Webb (1976, 1978*a*) to be an indicator of fast-start performance.

The difference in velocity and acceleration values during s2 can be reconciled with the difference in kinematics of the two C-start types. According to Weihs (1973), the highest forward acceleration should occur in stage 2 as a result of the return flip. Since SB responses show neither a clear return flip nor a body bend in the opposite direction to that of the initial one, it is not surprising that velocity and acceleration profiles differ from those of DB responses, which correspond kinematically to the description of a fast-start by Weihs (1973). Although average acceleration is negative during SB s2 (mean $-1.8\pm5.6\,m\,s^{-2}$), a small peak in acceleration is observed shortly after the end of s1 (Fig. 3C). The mean value of this peak is $34.07\pm12.7\,m\,s^{-2}$ (mean maximum acceleration s2 SB), which corresponds to about half the magnitude of DB s2, SB s1 and DB s1. This acceleration shows that there is some thrust being produced after the end of s1.

This study provides the first fast-start performance data on a paired-fin propulsion specialist. It is of interest to consider if this specialization impairs performance in body/caudal-fin fast-start swimming. Most previous studies have not made distinctions among C-start types. Therefore, we have compared DB responses and the pooled data (Table 3) with previous studies (Table 4). Velocities are given in actual values and as specific velocities ($L\,s^{-1}$), since fast-start velocity has been shown to increase with size (Webb, 1976). However, according to Webb (1976), acceleration performance is independent of size and so absolute values for acceleration rate are compared here. Maximum and mean values for specific velocity and acceleration rate of the angelfish fall in the high range, considering both DB responses and pooled performance values (Tables 3, 4). Film rates of 200–250 Hz give values most useful for comparison with ours. According to Harper and Blake (1989), these film rates should underestimate the instantaneous maximum acceleration by 20–30%. Given our estimated error of 8%, the angelfish maximum acceleration performance remains high. The relatively high velocity observed in angelfish is not surprising when they are compared with larger fish (Wardle, 1975). However, some of the fish listed in Table 4 are of very similar length to the ones we tested.

C-start types

Eaton *et al.* (1981) recognized a 'fast forward C-start', as opposed to C-starts in which the turn continued in the same direction through the response. Their criterion for discriminating between the two types is based on the change of direction during s2, whereas here DB s2 angle approaches zero as s1 angle increases beyond 90° (Fig. 4A); however, these large DB turns differ from SB turns, showing a higher degree of contralateral bending and bimodal distance–time profiles.

Previous studies (Eaton *et al.* 1977; Webb, 1976, 1978*a*; Dubois *et al.* 1976) have focused on fusiform fish, which employ axial locomotion for routine swimming.

Table 4. *Summary of previous fast-start studies; all values reported refer to C-type fast starts unless unspecified by the authors (1) or mean of pooled C and S starts (2)*

	Mean maximum acceleration (ms^{-2})	Mean acceleration rate (ms^{-2})	Mean maximum velocity		Mean velocity		Distance (m)	Time (s)	Species	Common name	Length (m)	Method	Rate (Hz)
			(ms^{-1})	(Ls^{-1})	(ms^{-1})	(Ls^{-1})							
Weihs (1973)	40.0	–	–		–				*Salmo trutta*	Trout	–	F	–
	50.0	–	–		–				*Esox* sp.	Pike	–	F	–
	25.5	20.6	–		0.57†	1.7	0.113‡	0 200‡	*Salmo gairdneri*	Rainbow trout	0 330	F	40
Webb (1975)	42.1	12.1	1.21	8.5	0.72†	5 0	0 056	0 078	*Salmo gairdneri*	Rainbow trout	0.143	F	64
	15.7	8.1	0 67	8 4	0.36†	4.5	0 029	0 079	*Lepomis cyanellus*	Green sunfish	0.080	F	64
	95 0	–	–		–		–	–	*Salmo gairdneri*	Rainbow trout*	–	F	64
Dubois *et al.* (1976)	23.5	–	2.80	4.4	–		–	0 210	*Pomotamus saltatrix*	Bluefish (1)*	0.630	A	
Webb (1976)	40.6	17 6	2 85	7 4	1 63†	4.2	0.163	0.100	*Salmo gairdneri*	Rainbow trout (2)	0.387	F	64
Webb (1977)	26 6	8.6	1 44	8.3	0 70†	4 0	0 076	0 109	*Salmo gairdneri*	Rainbow trout	0.174	F	250
Webb (1978*a*)	41 0	–	1.71	12.6	1 13†	8 3	0 113	0 100	*Salmo gairdneri*	Rainbow trout	0.136	F	250
Webb (1978*b*)	39.5	10.4	1 56	7 2	0.73	3.4	0.084‡	0 115‡	*Esox* sp	Tiger musky	0.217	F	250
	32.6	10.6	1.58	8.1	0 75	3.8	0 085‡	0 114‡	*Salmo gairdneri*	Rainbow trout	0.195	F	250
	23.9	9 3	1.15	7 4	0 50	3.2	0.051‡	0.103‡	*Perca flavescens*	Yellow perch	0.155	F	250
	28.8	12.3	1.30	8 5	0 67	4 4	0 059‡	0.088‡	*Lepomis macrochirus*	Bluegill	0.153	F	250
	28.7	11.0	1.14	10 7	0 49	4 6	0 038‡	0 078‡	*Notropis cornutus*	Common shiner	0.107	F	250
	22.7	6.1	0.77	9 4	0 43	5.2	0.035‡	0.081‡	*Cottus cognatus*	Slimy sculpin	0.082	F	250
	32 3	10 3	0.89	14 4	0.43	6.9	0.024‡	0 056‡	*Etheostoma caerulem*	Rainbow darter	0.062	F	250
Webb (1983)	80 0	–	2.50	9.7	–		–	–	*Salmo gairdneri*	Rainbow trout	0.257	F	60
	110.0	–	2.50	10 6	–		–	–	*Micropterus dolomieu*	Smallmouth bass	0.236	F	60
Webb (1986*a*)	–	16 0‡	–		–		–	–	*Esox* sp	Tiger musky	0.065	F	60
	–	15 0‡	0.96	18.8	–		–	–	*Micropterus salmoides*	Largemouth bass	0 051	F	60
	–	14.5‡	1.01	15.8	–		–	–	*Lepomis macrochirus*	Bluegill	0 064	F	60
	–	11.5‡	0.81	14.0	–		–	–	*Pimephales promelas*	Fathead minnow	0.058	F	60
Harper and Blake (1990)	56.6	21.4	2 79	8 8	1.16	3.6	0.141	0 134	*Salmo gairdneri*	Rainbow trout	0.318	A	
	157.8	54.7	4 70	12.4	2 27	6 0	0 194	0 085	*Esox lucius*	Pike	0 378	A	

* Single event; † calculated from data; ‡ read from figures.

A, accelerometer; F, film

Salmo gairdneri=*Oncorhynchus mykiss*.

The angelfish is specialized for low-speed swimming, employing pectoral fin rowing (Blake, 1979). Axial locomotion is only employed for fast-starts and rapid turning manoeuvres. This might account for its fast-start types and explain the presence of single bend and double bend C-starts, which highlight manoeuvrability and high speed, respectively.

The main difference between the two types of escape is in the intensity of the stage 2 return flip, which suggests that, in SB responses, stage 2 might not be a purely active process. Eaton *et al.* (1977) documented the occurrence of an escape response where stage 2 was absent in garfish (*Xenetodon cancila*). In this case the fish bent into a C during stage 1 and did not straighten the body subsequently. They suggested that this observation supports the idea that the return flip (s2) is an active process and not a passive mechanical consequence of rapid body bending (s1). However, the garfish is rather elongate and probably shows a passive recoil to a lesser extent than does the laterally compressed angelfish. In the absence of EMG data, we can only speculate that SB and DB responses might be the result of a differential contralateral muscular contraction, and passive recoil might play a different role in the two types. Eaton *et al.* (1988) suggested that a purely mechanical effect cannot entirely explain the s2 propulsion and observed two EMG signals, one associated with the s1 contraction and the second with the propulsive stroke during s2. However, the EMG data were not matched with distance–time data, and it is not possible to relate differences in acceleration profiles to the EMGs. In addition to differential contralateral contraction, the two types of C-start might differ in the relaxation phase of the initial contraction. Covell *et al.* (1991) observed that, during s2, the deformation curve of ultrasonic dimension gauges implanted on the side of the initial contraction varied both with the location of the gauge and with the nature of the response.

General conclusions

Webb (1984) classified fish swimming styles into three broad categories: body/caudal-fin (BCF) periodic (cruising) propulsion; BCF transient (fast-start) propulsion; median- and paired-fin (MPF) propulsion, used in slow and precise manoeuvres. It has been suggested that specialization for locomotion performance in any one area is usually associated with reduced performance in one or more of the others (Webb, 1984). This study suggests that optimal morphology for MPF propulsion does not impair performance at the BCF transient level. Optimal design for BCF transient propulsion has been suggested to involve a large body depth (especially caudally), a flexible body and a large muscle mass relative to body mass (Webb, 1984). The angelfish possesses two of these specializations. Its fineness ratio (L/D, where D is body depth) is amongst the lowest of all fishes (Aleev, 1969) and its body surface area in relation to its length is higher ($S_w=1.02L^2$) than in any other species studied. High flexibility associated with extreme lateral compression allows the angelfish to perform very tight turns when escaping. Although the value of muscle mass relative to body mass is lower

(0.39*M*) than in fast-start specialists (e.g. pike, 0.55*M*; Webb, 1978*a*), it is comparable to that of many generalist fish (Webb, 1978*a*).

The angelfish is well designed for two different locomotor modes, which are employed in different situations (feeding at low speed, acceleration to escape predators). During low-speed swimming, the body is kept rigid and the pectoral fins are moved by aerobic musculature. In contrast, during fast-starts, the body is bent, employing the anaerobic axial musculature.

Within its fast-start capabilities, the angelfish has two options. Escape responses of the SB type highlight manoeuvre, by allowing the body contraction to continue in only one direction, resulting in turns, whereas in DB responses the initial contraction is compensated by one in the opposite direction, resulting in a more linear trajectory. In the latter case, a higher velocity, given by a double acceleration, is achieved (Fig. 7). Further studies would be required to clarify the mechanism underlying this differential pattern of behaviour and its biological significance. Perhaps there are behavioural trade-offs between high distance–time performance and large turns, such that the prey would employ a particular type of response depending on the predator's strike tactics.

Fig. 8A shows the ranges of s1 turning angle observed for both types of

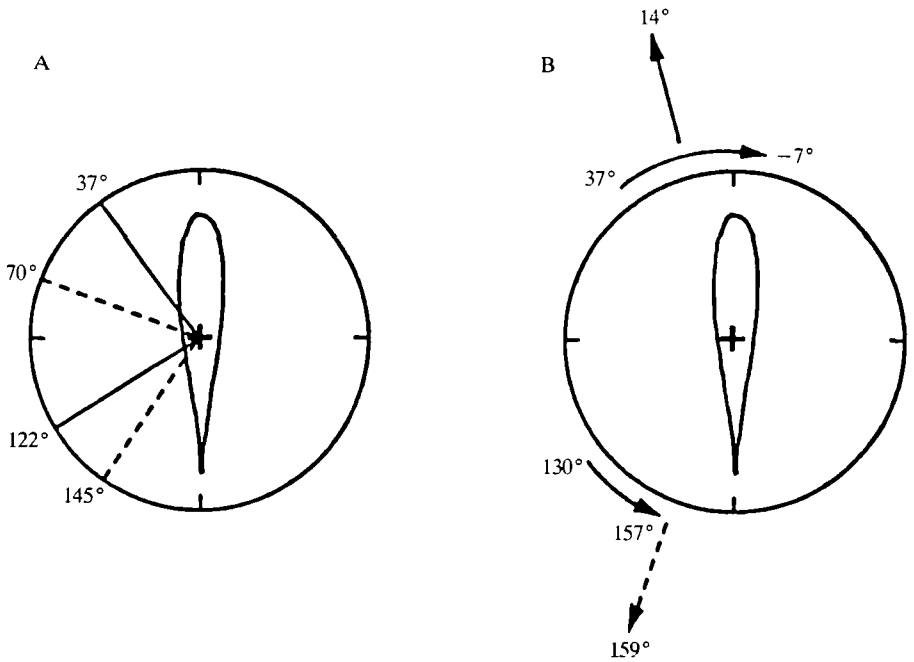

Fig. 8. (A) Range of s1 turning angles for double bend (continuous line) and single bend (dotted line) responses. (B) Overall range of total escape angles given by a double bend (continuous straight arrow) and a single bend (dotted straight arrow) response. Curved arrows indicate the change in direction between s1 and s2 turning angles.

response. Combined, the two ranges would allow a total range of angles of turn between 37 and 145°. These values might not be the actual limits of the angelfish s1 turning angles. However, a lower limit, set by the s1 contraction, and an upper limit, set by limited body flexibility, are likely. Since survival depends on the ability of the fish to escape dangers from all directions, it would be important to have the widest range of turning trajectories available on each side. This might be achieved only when employing DB escapes for small turns and SB escapes for large turns (Fig. 4B). The new limits when considering the total escape angle are much wider (14–159°; Fig. 8B) and result, respectively, from contralateral bending (DB) and a continuation of the turn (SB) during s2. Arguably, the choice of C-start type might be important in determining the escape trajectory to avoid predators.

We would like to thank Drs J. M. Gosline, J. Matsubara and D. Harper and Mr R. Frith for constructive comments on this project and Messrs M. Smith, A. Parker, M. Kasapi and D. Montagnes and Ms T. Sutherland for help in the data analysis. The Natural Science and Engineering Research Council provided financial support. We would also like to thank two anonymous referees for their valuable comments on an earlier draft of this paper. This work was completed while RWB was a Killam Research Fellow at the University of British Columbia and PD was in receipt of a Fondazione Rui Graduate Scholarship.

References

ALEEV, YU G. (1969). *Function and Gross Morphology in Fish.* Jerusalem: Kater Press.

BLAKE, R. W. (1979). The mechanics of labriform locomotion. I. Labriform locomotion in the angelfish (*Pterophyllum eimekei*): an analysis of the power stroke. *J. exp. Biol.* **82**, 255–271.

BLAKE, R. W. (1983). *Fish Locomotion.* Cambridge: Cambridge University Press. 208pp.

BLAXTER, J. H. S., GRAY, J. A. B. AND DENTON, E. J. (1981). Sound and startle responses in herring shoals. *J. mar. biol. Ass. U.K.* **61**, 851–869.

COVELL, W. C., SMITH, D. M., HARPER, D. AND BLAKE, R. W. (1991). Skeletal muscle deformation in the lateral muscle of the intact rainbow trout *Salmo gairdneri* during fast-start maneuvers. *J. exp. Biol.* **156**, 453–466.

DANIEL, T. L. (1984). Unsteady aspects of aquatic locomotion. *Am. Zool.* **24**, 121–134.

DIDOMENICO, R., NISSANOV, J. AND EATON, R. C. (1988). Lateralization and adaptation of a continuously variable behavior following lesions of a reticulospinal command neuron. *Brain Res.* **473**, 15–28.

DUBOIS, A. B., CAVAGNA, G. A. AND FOX, R. S. (1976). Locomotion of bluefish. *J. exp. Zool.* **195**, 223–226.

EATON, R. C., BOMBARDIERI, R. A. AND MEYER, D. H. (1977). The Mauthner initiated startle response in teleost fish. *J. exp. Biol.* **66**, 65–81.

EATON, R. C., DIDOMENICO, R. AND NISSANOV, J. (1988). Flexible body dynamics of the goldfish C-start: implication for reticulospinal command mechanisms. *J. Neurosci.* **8**, 2758–2768.

EATON, R. C. AND HACKETT, J. T. (1984). The role of Mauthner cell in fast-starts involving escape in teleost fish. In *Neural Mechanisms of Startle Behavior* (ed. R. C. Eaton), pp. 213–266. New York: Plenum Press.

EATON, R. C., LAVENDER, W. A. AND WIELAND, C. M. (1981). Identification of Mauthner-initiated response pattern in goldfish: Evidence from simultaneous cinematography and electrophysiology. *J. comp. Physiol.* **144**, 512–531.

EATON, R. C., NISSANOV, J. AND WIELAND, C. M. (1984). Differential activation of Mauthner

and non-Mauthner startle circuits in the zebrafish: Implication for functional substitution. *J. comp. Physiol.* A **155**, 813–820.

GILLETTE, R. (1987). The role of neuronal command in fixed action pattern of behavior. In *Aim and Methods in Neuroethology* (ed. D. M. Guthrie), pp. 46–79. Manchester: Manchester University Press.

HARPER, D. G. AND BLAKE, R. W. (1989). On the error involved in high-speed film when used to evaluate maximum acceleration of fish. *Can. J. Zool.* **67**, 1929–1936.

HARPER, D. G. AND BLAKE, R. W. (1990). Fast-start performance of rainbow trout *Salmo gairdneri* and northern pike *Esox lucius*. *J. exp. Biol.* **150**, 321–342.

HOWLAND, H. C. (1974). Optimal strategies for predator avoidance: The relative importance of speed and manoeuvrability. *J. theor. Biol.* **134**, 56–76.

LANCZOS, C. (1956). *Applied Analysis*. Englewood Cliffs, New Jersey: Prentice Hall.

NISSANOV, J. AND EATON, R. C. (1989). Reticulospinal control of rapid escape turning manoeuvres in fishes. *Am. Zool.* **29**, 103–121.

SCHULTZ, L. P. (1967). Review of South American freshwater angelfish – genus *Pterophyllum*. *Proc. U.S. natn. Mus.* **120**, 1–10.

WARDLE, C. S. (1975). Limit of fish swimming speed. *Nature* **255**, 725–727.

WEBB, P. W. (1975). Acceleration performance of rainbow trout *Salmo gairdneri* and green sunfish *Lepomis cyanellus*. *J. exp. Biol.* **63**, 451–465.

WEBB, P. W. (1976). The effect of size on fast-start performance of rainbow trout *Salmo gairdneri*, and a consideration of piscivorous predator–prey interaction. *J. exp. Biol.* **65**, 157–177.

WEBB, P. W. (1977). Effects of median fin amputation on fast-start performance of rainbow trout (*Salmo gairdneri*). *J. exp. Biol.* **68**, 123–135.

WEBB, P. W. (1978*a*). Fast-start performance and body form in seven species of teleost fish. *J. exp. Biol.* **74**, 211–226.

WEBB, P. W. (1978*b*). Temperature effects on acceleration of rainbow trout *Salmo gairdneri*. *J. Fish. Res. Bd Can.* **35**, 1417–1422.

WEBB, P. W. (1982). Avoidance responses of fathead minnow to strikes by four teleost predators. *J. comp. Physiol.* **147**, 371–378.

WEBB, P. W. (1983). Speed, acceleration, and manoeuvrability of two teleost fishes. *J. exp. Biol.* **102**, 115–122.

WEBB, P. W. (1984). Body form, locomotion and foraging in aquatic vertebrates. *Am. Zool.* **24**, 107–120.

WEBB, P. W. (1986*a*). Effect of body form and response threshold on the vulnerability of four species of teleost prey attacked by largemouth bass. *Can. J. Fish. aquat. Sci.* **43**, 763–771.

WEBB, P. W. (1986*b*). Locomotion and predator–prey relationship. In *Predator–Prey Relationships* (ed. G. V. Lauder and M. E. Feder), pp. 24–41. Chicago: University of Chicago Press.

WEBB, P. W. AND BLAKE R. W. (1985). Swimming. In *Functional Vertebrate Morphology* (ed. M. Hildebrand, D. M. Bramble, K. Liem and D. B. Wake), pp. 110–128. Cambridge, MA: Harvard University Press.

WEBB, P. W. AND KEYES, R. S. (1981). Division of labour between median fins in swimming dolphin (Pisces: Coryphaenidea). *Copeia* **1981**, 901–904.

WEIHS, D. (1973). The mechanism of rapid starting of slender fish. *Biorheology* **10**, 343–350.

WEIHS, D. AND WEBB, P. W. (1984). Optimal avoidance and evasion tactics in predator–prey interactions. *J. theor. Biol.* **63**, 451–465.